

**Uridine Binding and Transportability Determinants of Human Concentrative
Nucleoside Transporters**

Jing Zhang, Kyla M. Smith, Tracey Tackaberry, Frank Visser, Morris J. Robins, Lars P.C.
Nielsen, Ireneusz Nowak, Edward Karpinski, Stephen A. Baldwin, James D. Young, and
Carol E. Cass

Department of Oncology, University of Alberta, and the Cross Cancer Institute,
Edmonton, Alberta T6H 1Z2, Canada

Running title: Uridine recognition and transportability motifs of hCNTs

Address correspondence to: Dr. Carol E. Cass, Department of Oncology, University of Alberta, Cross Cancer Institute, 11540 University Ave., Edmonton, Alberta, Canada T6H 1Z2 (Tel: 780-432-8320; Fax: 780-432-8425; email: carol.cass@cancerboard.ab.ca)

The number of text pages: 22

The number of tables: 2

The number of figures: 4

The number of references: 30

The number of words in the *Abstract*: 244

The number of words in the *Introduction*: 710

The number of words in the *Discussion*: 1230

The abbreviations used are: CNT, concentrative nucleoside transporter; ENT, equilibrative nucleoside transporter; DMSO, dimethyl sulfoxide; h, human; CMM, complete minimal media; GLU, glucose; IC₅₀, inhibitory concentration 50%; K_i, inhibitory constant; ΔG^0 , Gibbs free energy; TTBS, 0.2% Tween-20, Tris-buffered saline; Nucleoside names and abbreviations are listed in Table 1.

Abstract

Human concentrative nucleoside transporters 1, 2 and 3 (hCNT1, hCNT2 and hCNT3) exhibit different functional characteristics and a better understanding of their permeant selectivities is critical for development of nucleoside analog drugs with optimal pharmacokinetic properties. In this study, the sensitivity of a high throughput yeast expression system used previously for hCNT1 and hCNT3 was improved and used to characterize determinants for interaction of uridine (Urd) with hCNT2. The observed changes of binding energy between hCNT2 and different Urd analogs suggested that it interacts with C(3')-OH, C(5')-OH and N(3)-H of Urd. The C(2') and C(5) regions of Urd played minor but significant roles for Urd-hCNT2 binding, possibly through Van der Waals interactions. Since the yeast assay only provided information about potential transportability, the permeant selectivities of recombinant hCNT1, 2 and 3 produced in oocytes of *Xenopus laevis* were investigated using a two-electrode voltage clamp assay. hCNT1-mediated transport was sensitive to modifications of the N(3), C(3') and C(5') positions of Urd. hCNT2 showed some tolerance for transporting Urd analogs with C(2') or C(5) modifications, little tolerance for N(3) modifications and no tolerance for any modifications at C(3') or C(5') of uridine. Although hCNT3 was sensitive to C(3') modifications, it transported a broad range of variously substituted Urd analogs. The transportability profiles identified in this study, which reflected well the binding profiles, should prove useful in the development of anti-cancer and antiviral therapies with nucleoside drugs that are permeants of members of the hCNT protein family.

Introduction

Mammalian nucleoside transporters are classified into two structurally and mechanistically unrelated protein families, the concentrative and equilibrative nucleoside transporters (CNTs and ENTs) (Baldwin et al., 1999; Cass et al., 1999). The ENTs transport a broad range of purine and pyrimidine nucleosides down their concentration gradients, whereas the CNTs couple uphill nucleoside transport to downhill sodium transport and, in the case of hCNT3, also proton transport. Three human (h) CNTs with different permeant selectivities have been identified by molecular cloning and functional expression in oocytes of *Xenopus laevis* (Ritzel et al., 1997; Ritzel et al., 1998; Ritzel et al., 2001). hCNT1 and hCNT2 prefer pyrimidine nucleosides and purine nucleosides, respectively, although hCNT1 also transports adenosine and hCNT2 also transports uridine (Urd). hCNT3 transports a broad range of pyrimidine and purine nucleosides (Ritzel et al., 2001; Zhang et al., 2003). The ENTs appear to be expressed in most human cell types. In contrast, the CNTs are found primarily in specialized cell types, including renal and gastrointestinal epithelia (del Santo et al., 2001; Li et al., 2001; Ngo et al., 2001; Ritzel et al., 1998; Ritzel et al., 2001), suggesting an important role in absorption, secretion, distribution and elimination of physiologic nucleosides and nucleoside drugs. hCNTs have also been observed in leukemic cells and a few cancer cell lines (Garcia-Manteiga et al., 2003; Mackey et al., 1998; Ritzel et al., 2001). Differences in tissue distribution and permeant selectivities of hCNTs suggest different nucleoside-transport capacities of various tissues and distinct physiological and pharmacological roles.

Nucleoside analogs are used clinically in the treatment of cancer and viral infections. Understanding the structural requirements for transporter binding and

translocation of nucleosides should enable the design of more effective strategies for use of therapeutic nucleosides. In the absence of detailed structures for nucleoside transporter proteins, several experimental approaches have been used to define the structural requirements of nucleosides for interaction with the transporters (Chang et al., 2004; Lang et al., 2001; Lang et al., 2004; Patil et al., 2000). A study with human intestinal brush border membrane vesicles suggested that the binding sites of hCNT1 and hCNT2 differentially interacted with analogs of their common permeants, uridine and adenosine (Patil et al., 2000). Using three-dimensional quantitative structure-activity relationships that were based on inhibition data obtained previously, this same group generated pharmacophore models in which the predominant determinants for ligand interaction were hydrogen bonding for hCNT2 and electrostatic and steric features for hCNT1 and hENT1 (Chang et al., 2004). In a study with stably transfected human cell cell lines, hCNT1 and hCNT2 exhibited different capacities for binding of uridine and adenosine analogs with substituents on the ribosyl and/or base moieties (Lang et al., 2001; Lang et al., 2004). A high-throughput inhibitor-sensitivity assay in which recombinant hCNT1, hCNT3, hENT1, and hENT2 were produced in yeast was used to quantify the inhibitory effects of Urd analogs with systematic sugar modifications (Vickers et al., 2004; Zhang et al., 2003). A common observation in all of these inhibition studies was the importance of the 3'-hydroxyl group for high affinity interaction of permeants and/or inhibitors with the transporters.

A deficiency of the approaches taken thus far to define the structural determinants for interaction of nucleoside analogs with the transporters is that they are based primarily on inhibition data. The current work was undertaken to extend our earlier inhibition studies of Urd binding motifs with hCNT1 and hCNT3 (Zhang et al., 2003) to include

hCNT2, which was not utilized previously because of its low expression levels in the yeast strain initially used in the inhibition assay, and to determine the extent to which the inhibitory uridine analogs were also permeants. The original difficulty of hCNT2 production was circumvented by introducing the hCNT2-containing plasmid into a double knockout yeast strain (*fui1::HIS3*) that lacked both Urd permease (*Fui1*) and uracil permease (*Fur4*). The binding motif of hCNT2 exhibited distinct features when compared with hCNT1 and hCNT3. Since a high-affinity ligand may inhibit nucleoside transport without also being transported, two-voltage clamp experiments were performed in *Xenopus laevis* oocytes to determine if the Urd analogs that inhibited Urd transport were also permeants, thus defining the transportability profiles of hCNT1, hCNT2 and hCNT3. Each hCNT exhibited a distinct Urd transportability profile that was closely related to its permeant binding profile.

Material and Methods

Strains and media

BY4742-YBR021W (*MAT α* , *his3*, *leu2*, *lys2*, *ura3*, Δ *FUR4*), which contains a disruption in the gene encoding the endogenous uracil permease, *FUR4*, was purchased from American Type Culture Collection (Manassas, VA) and used as the parental yeast strain to generate the double knockout strain *fui1::HIS3*. *Fui1::HIS3* was generated by deleting the *FUR4* gene using the polymerase chain reaction (PCR)-mediated one-step gene disruption method (Winzeler et al., 1999). Other strains were generated by transformation of the yeast-*Escherichia coli* shuttle vector pYPGE15 (Brunelli, 1993) into *Fui1::HIS3* using a standard lithium acetate method (Ito et al., 1983).

The gene locus for FUI1 was disrupted by integration of the HIS3 expression cassette, encoding imidazoleglycerolphosphate dehydratase (EC 4.2.1.19) into the coding region of the FUI1 gene to create *fui1::HIS3*. The *fui1*-disruption mutants were selected in a medium that lacked histidine but contained 500 μ M FUrD. Since Fui1-mediated transport of FUrD leads to yeast death (Vickers et al., 2000), survival in 500 μ M FUrD indicated the successful targeted integration of the HIS3 cassette into the yeast genome with disruption of the Fui1 gene. Three of the surviving yeast colonies and BY4742-YBR021W were then tested for their abilities to transport [3 H]uracil or [3 H]Urd in the presence and absence of either 5 or 10 mM non-radioactive uracil or Urd, respectively.

Yeast strains were maintained in complete minimal media (CMM) containing 0.67% yeast nitrogen base (Difco, Detroit MI), amino acids (as required to maintain auxotrophic selection), and 2% glucose (CMM/GLU). Agar plates contained CMM with various supplements and 2% agar (Difco). Plasmids were propagated in *E. coli* strain TOP10F' (Invitrogen, Carlsbad, CA) and maintained in Luria broth with ampicillin (100 μ g/ml).

DNA manipulation and plasmid construction

To construct the deletion strain *Fui1::HIS3*, two 71-mer oligonucleotide primers were synthesized (Invitrogen, Carlsbad, CA), each containing (3' to 5') 21 bases of homology to the HIS3 cassette, a unique 50-bp tag sequence that was complementary to the region (either upstream or downstream of the *fui1* open reading frame) being targeted (including the start or stop codon). The 71-mer primers were used to amplify the HIS3 gene cassette, which was contained in plasmid pJJ215 (a generous gift from Dr. B. Lemire, University of Alberta, Edmonton, AB). The amplified PCR products were transformed into BY4742-YBR021W using the lithium acetate method and the resulting

transformed yeast were selected by growing on agar plates that contained 500 μ M FUrD but lacked histidine.

For *S. cerevisiae* expression, the hCNT2 open reading frames were amplified from vectors (pCDNA3-hCNT2) by PCR methodology using the following primers (restriction sites underlined): 5'-XbaI-hCNT2 (5'-CTG TCT AGA ATG GAG AAA GCA AGT GGA AG-3'), 3'-KpnI-hCNT2 (5'-CGA GGT ACC TCA GGC ACA GAC GGT ATT GTT GTA G -3'). The amplified open reading frames were inserted into pYPGE15 (a high copy-number episomal yeast vector that expresses the inserted DNA constitutively under the transcriptional control of the phosphoglycerate kinase promoter) to generate pYPhCNT2. The PCR reactions were performed using *Pwo* polymerase (Roche Molecular Biochemicals, Indianapolis, IN) and the resulting PCR products were verified by DNA sequencing using an ABI PRISM 310 sequence detection system (PerkinElmer Life Sciences, Norwalk, CT).

Immunostaining of yeast membranes

Yeast membranes were prepared by a previously described method (Vickers et al., 2000) and subjected to SDS-polyacrylamide gel electrophoresis (Vickers et al., 1999), after which proteins were transferred to polyvinylidene fluoride membranes (Immobilon-P, Millipore, Bedford, MA). The transfer membranes were blocked overnight at 4°C first in TTBS (0.2% Tween-20, Tris-buffered saline) containing 5% (w/v) skim milk powder and then in TTBS with antibodies against hCNT2 and 5% (w/v) skim milk powder. The membranes were then washed three times with TTBS, incubated with TTBS-containing species-specific horseradish-peroxidase secondary antibodies (Jackson ImmunoResearch Laboratories Inc., West Grove, PA) and 5% (w/v) skim milk powder, washed with TTBS, and visualized with enhanced chemiluminescence (ECL, Amersham Pharmacia Biotech)

and autoradiography. Monoclonal antibodies against hCNT2 were raised by established methods (Jennings et al., 2001) against an immunogenic epitope that corresponded to residues 30-51 of hCNT2, a region predicted to be located in a large intracellular loop close to the amino terminus. The conjugated and unconjugated synthetic peptides were obtained from the Alberta Peptide Institute (Edmonton, Canada).

Urd uptake in yeast producing recombinant hCNT2

The uptake of [³H]Urd, [³H]adenosine, [³H]cytidine and [³H]inosine (Moravek Biochemicals, Brea, CA) into logarithmically proliferating yeast was measured using a cell harvester as described previously (Vickers et al., 2002; Zhang et al., 2003). Briefly, yeast were grown in CMM/GLU to an OD₆₀₀ of 0.8-1.2, washed three times with fresh CMM/GLU (pH 7.4), and re-suspended to an OD₆₀₀ of 4 in CMM/GLU (pH 7.4). Fifty- μ l portions of CMM/GLU (pH 7.4) with [³H]Urd and a test compound (if present) at twice the desired concentration were preloaded into 96-well plates. The transport assays were initiated by adding equal volume of yeast suspension at OD₆₀₀ = 4 to the individual wells of the preloaded 96-well plates, which were placed on the semi-automated cell harvester (Micro96TM HARVESTER, Skatron Instruments, Norway). At graded time intervals, groups of transport reactions (usually 24) were terminated simultaneously by harvesting yeast on glass-fiber filters (Skatron Instruments) with continued washing with demineralized water to remove unincorporated permeant. The filter discs with yeast corresponding to a particular transport assay were placed into individual scintillation counting vials (one disc/vial) to which 5 ml of scintillation counting fluid (EcoLite) was added. Scintillation vials were allowed to sit at room temperature overnight with shaking before analysis.

The binding of Urd and its analogs to recombinant hCNT2 was assessed by measuring their abilities to inhibit the uptake of [³H]Urd in the “inhibitor-sensitivity” assay as follows. Yeast were incubated with graded concentrations of a particular test compound and 1 μM [³H]Urd in CMM/GLU (pH 7.4) for 20 min after which [³H]Urd uptake was measured. All experiments were carried out in quadruplicate. The amount of [³H]Urd associated with yeast in the presence of 10 mM non-radioactive Urd was also determined to quantify non-specifically associated radioactivity, which was subtracted from total radioactivity for each transport assay. Data were fitted to theoretical inhibition curves by nonlinear regression to obtain IC₅₀ values (concentrations that inhibited reactions by 50%). K_i (inhibitory constant) values were determined from the equation (Cheng and Prusoff, 1973) in which $K_i = IC_{50}/[1 + (L/K_m)]$ and L = [³H]Urd concentration, which was always 1 μM. Gibbs free energy (ΔG^0) was calculated from $\Delta G^0 = -RT\ln(K_i)$, in which R is the gas constant and T is the absolute temperature. The thermodynamic stability of transporter-inhibitor complexes was quantitatively estimated from ΔG^0 as described elsewhere (de Koning and Jarvis, 2001).

Steady-state electrophysiological studies

hCNT1, hCNT2 or hCNT3 cDNA in pGEM-HE (Ritzel et al., 1997; Ritzel et al., 1998; Ritzel et al., 2001) was linearized with *Nhe1* and transcribed with T3 or T7 polymerase using the mMESSAGING mMACHINE™ (Ambion, Austin, TX) transcription system. *In vitro* synthesized transcripts were injected into isolated mature stage VI oocytes from *X. laevis* as described previously (Smith et al., 2004). Mock-injected oocytes were injected with water alone.

Oocyte membrane currents were measured using a GeneClamp 500B oocyte clamp (Axon Instruments, Inc., Foster City, CA, USA) in the two-electrode, voltage-clamp mode as described previously (Smith et al., 2004). All experiments were performed at room temperature (20°C) and oocytes were discarded if membrane potentials were unstable or more positive than -30 mV. The membrane potential was clamped at a holding potential of -50 mV and Urd or Urd analogs were added at various concentrations. The sodium currents induced by 100 μ M Urd were used as controls to compare the transportability of Urd analogs by recombinant hCNT1, hCNT2 and hCNT3. The concentrations of Urd analogs for electrophysiological studies were chosen based on their K_i values for inhibition of hCNT1 and hCNT3 (Zhang et al., 2003) and hCNT2 (this study) as determined in the inhibitor-sensitivity assay. The transport medium contained (mM): NaCl, 100; KCl, 2; CaCl₂, 1; MgCl₂, 1; HEPES, 10 (pH 7.5). Current values are presented as means \pm S.E of three or more oocytes.

Urd analogs

The structures of Urd and its analogs were given previously (Vickers et al., 2004; Zhang et al., 2003). The abbreviations of Urd analogs are given in Table 1. The Urd analogs used in this study were either obtained from R. I. Chemical, Inc. (Orange, CA) or were synthesized as described elsewhere (Zhang et al., 2003).

Stock solutions of test compounds were either prepared in water or dimethyl sulfoxide (DMSO) (Sigma) and the final concentration of DMSO in transport reactions was 0.1% if DMSO was used as a solvent.

Results

Detection of recombinant hCNT2 in yeast membranes. The production of recombinant hCNT2 in *S. cerevisiae* was verified by immunoblotting using anti-hCNT2 antibodies (Fig. 1, Panel A). A 75-kDa immunoreactive species was detected in membranes of pYPhCNT2-containing yeast and was not detected in membranes of pYPGE15-containing yeast (Fig. 1, Panel A). The electrophoretic mobilities of the detected proteins were consistent with the predicted molecular mass of hCNT2.

Urd transport by recombinant hCNT2 produced in yeast. The *fui1*, *fur4* double knockout strain (*fui1::HIS3*) was confirmed by demonstrating that it was unable to transport either [³H]Urd or [³H]uracil. The parental strain (BY4742-YBR021W) exhibited Urd, but not uracil, transport activity (data not shown).

The time course for uptake of 1 μ M [³H]Urd into *fui1::HIS3* that contained pYPGE15 was linear over extended periods (> 30 min) and exhibited rates of 0.05 ± 0.01 and 0.04 ± 0.01 pmol/mg protein/min in the presence and absence of 10 mM cold uridine, respectively (data not shown). When time courses for influx of 1 μ M [³H]Urd were measured in the presence and absence of 10 mM non-radioactive Urd into *fui1::HIS3* yeast that contained pYPhCNT2 (Fig. 1, Panel B), the time courses were linear for up to 30 min with mean rates (\pm S.E.) of 4.1 ± 0.09 and 0.05 ± 0.02 pmol/mg protein/min, respectively, indicating the presence of functional hCNT2 in yeast plasma membranes. Urd transport rates were determined for all subsequent experiments using incubation times of 20 min for recombinant hCNT2 produced in yeast, thereby providing large signal-to-noise ratios and maintaining initial rates of uptake. Results from similar experiments with other ³H-labeled nucleosides demonstrated that recombinant hCNT2

also transported adenosine, inosine and guanosine, but not cytidine and Thd (data not shown), confirming that the permeant selectivity of recombinant hCNT2 produced in yeast was similar to that reported previously in cultured cells and *X. laevis* oocytes (Lang et al., 2001; Lang et al., 2004; Ritzel et al., 1998), thus providing a good model system for structure-function studies.

The experiments of Fig. 1, Panel C showed that recombinant hCNT2 had a moderate apparent affinity and capacity for Urd uptake ($K_m = 29 \pm 7 \mu\text{M}$, $V_{\text{max}} = 146 \pm 11 \text{ pmol/mg protein/min}$; mean \pm S.E., $n = 3$). The K_m value of recombinant hCNT2 was slightly lower than those obtained with *X. laevis* oocytes ($40 \pm 6 \mu\text{M}$, (Ritzel et al., 1998) and cultured mammalian cells (Lang et al., 2001; Ritzel et al., 1998); these differences are believed to be due to variations in post-translational modifications in the different expression systems and/or differences in membrane lipid environment (Visser et al., 2005).

Interaction of Urd analogs with recombinant hCNT2: inhibitor-sensitivity assays. To gain an understanding of the structural regions of Urd that interact with hCNT2, Urd analogs with modifications of the base and/or sugar moieties were tested systematically by assessing the concentration dependence of inhibition of transport of $1 \mu\text{M}$ Urd mediated by hCNT2. The inhibition of Urd uptake was assumed to be competitive since (i) the inhibitors tested were close structural analogs of Urd, and (ii) the transporter under study was most likely to be the sole source of interaction with the potential inhibitor. Representative concentration-effect curves of some of the analogs for inhibition of hCNT2-mediated Urd transport are shown in Fig. 2. In all cases, the Hill coefficients were close to -1 (mean \pm S.E. = -0.9 ± 0.2), indicating a single class of

inhibitor binding sites. The mean K_i values (\pm S.E.) and the corresponding Gibbs free energy values are listed in Table 1.

Base modifications. There were apparent weak interactions between hCNT2 and C(5) of Urd since the addition of larger substituents at the C(5) position resulted in decreases of 2-6 kJ/mol in ΔG° with 2-15 fold increases in K_i values. The K_i values increased dramatically with the increase in volume of the substituent (e.g., fluoro < bromo < iodo) at C(5); FUrd exhibited a K_i value of $61 \pm 13 \mu\text{M}$, twice that of Urd ($28 \pm 3 \mu\text{M}$), and IUrd exhibited a K_i value of $359 \pm 50 \mu\text{M}$, with a loss of 5.7 kJ/mol in ΔG° , suggesting that the interactions between hCNT2 and C(5) were steric. Although these interactions were not tight, high concentrations of FUrd, IUrd, and BrdUrd were capable of completely inhibiting hCNT2-mediated transport of Urd. Thd was a weak inhibitor of Urd uptake with a K_i value of $566 \pm 20 \mu\text{M}$. The lower affinities for FdUrd, BrdUrd, IdUrd and EtdUrd, with ΔG° values of 8-20 kJ/mol, as compared to 2'dUrd, suggested that the ethyl and iodo substituents, with larger sizes than the fluoro and bromo substituents, may have sterically reduced the ability of the analog to efficiently contact the transporter protein.

The 3 position of the base moiety (N(3)-H) contributed a recognition determinant for binding to hCNT2. The low affinity of 3MeUrd, with a 20-fold increase in K_i value compared to that of Urd, indicated the importance of the N(3) position as part of the binding motif, with a difference of 7 kJ/mol binding energy, suggesting loss of a weak hydrogen bond.

Sugar modifications. hCNT2 displayed a reduced affinity for 2'dUrd relative to Urd (Fig. 3) with a small loss of free energy ($\delta(\Delta G^\circ) = 2.1 \text{ kJ/mol}$). However, C(2') was

an important determinant for high-affinity binding of Urd by hCNT2 since other modifications at this position reduced interactions with hCNT2. The inverted orientation of the hydroxyl group produced an analog that could no longer interact with hCNT2 since AraU, an epimer of Urd with the 2'-hydroxyl group above the plane of the sugar ring, exhibited a pronounced reduction in its interaction with the transporter ($K_i > 3$ mM). Compounds with substitution of an O-methyl or azido group for the 2'-hydroxyl group failed to inhibit hCNT2-mediated Urd transport at high concentrations ($K_i > 3$ mM), most likely because of the bulkier size of the C(2')-O-CH₃ and C(2')-N₃ substituents.

Strong interactions existed between hCNT2 and C(5')- and C(3')-OH moieties since the removal of either the 5'- or 3'-hydroxyl groups yielded K_i values > 3 mM, with losses of >10.5 kJ/mol in ΔG^0 , suggesting that hydrogen bonding was important. Although 2'dUrd was a moderate-affinity inhibitor of hCNT2-mediated Urd transport, additional removal of the 3'- or 5'-hydroxyl groups diminished its inhibitory effects. The possible involvement of the 3'- and 5'-hydroxyl groups was also apparent from the effects of substitution of an azido or O-methyl group at these positions; hCNT2-mediated Urd transport remained unchanged in the presence of high concentrations of 3'AzdUrd, 3'OMeUrd, 5'AzdUrd or 5'OMeUrd. AZT, which is 3'-azido-3'-deoxythymidine, failed to inhibit hCNT2-mediated Urd uptake. The loss of more than 8 kJ/mol in ΔG^0 value upon substitution of a chloro group at the C(5') of 5'dUrd suggested the loss of hydrogen bonding between Urd and hCNT2. Although hCNT2 strongly bound Urd with the 3'-hydroxyl group below the sugar ring plane, its affinity for xyloU, with the 3'-hydroxyl group oriented upwards, was greatly reduced ($K_i > 3$ mM). Similarly, iPUrd failed to

inhibit Urd transport, presumably due to the presence at the 3' position of the isopropylidene group.

Permeant selectivities of hCNT1, hCNT2 and hCNT3 for uridine analogs: transport assays. To determine if the Urd analogs that bound to either hCNT1 (Zhang et al., 2003), hCNT3 (Zhang et al., 2003) or hCNT2 (this study) were also permeants, two-electrode voltage clamp studies were used to measure their abilities to induce inward sodium currents in oocytes of *X. laevis* producing each of the transporters. Currents produced by Urd, 2'dUrd, 3'dUrd and 5'dUrd in a sodium-containing medium are shown in Fig. 3. Average current values for Urd analogs with base modifications observed in oocytes injected with transcripts are shown in Fig. 4. To compare the transportability of Urd and Urd analogs, the mean values of Urd analog-induced currents were normalized to the mean values of Urd-produced currents and summarized as $I_{\text{Analog}}/I_{\text{Urd}}$ in Table 2 for hCNT1, hCNT2 and hCNT3. hCNT1 and hCNT2 generated similar inward currents ($I_{\text{Na}} = 140 \text{ nA}$) while hCNT3 induced higher currents ($I_{\text{Na}} = 330 \text{ nA}$) in the presence of $100 \mu\text{M}$ Urd. In all cases, the inward-directed sodium currents were reversible and abolished in a sodium-free medium and no steady-state currents were observed in control water-injected oocytes (data not shown).

Base modifications. Moderate currents ($I_{\text{Analog}}/I_{\text{Urd}} = 20\sim 60\%$) were elicited by hCNT1 and hCNT3 upon application of various concentrations of FUrd, IUrd, MeUrd and BrUrd whereas hCNT2 exhibited greatly reduced ability to transport Urd analogs with modifications at C(5), following a trend of diminished transportability with bulkier substituents [i.e., Urd ($100 \mu\text{M}$) > FUrd (50 and $100 \mu\text{M}$) > MeUrd ($500 \mu\text{M}$) > IUrd and BrUrd ($500 \mu\text{M}$)]. Unlike hCNT1 and hCNT2, hCNT3 transported 3MeUrd well at higher concentrations ($I_{\text{analog}}/I_{\text{Urd}} = 48\%$, $500 \mu\text{M}$ of 3MeUrd).

Sugar modifications. Moderate to large inward currents were elicited by hCNT1 with application of 2'dUrd or 5'dUrd (Fig. 3). The slightly higher currents of hCNT1 ($I_{\text{analog}}/I_{\text{Urd}} = 112\%$) observed with 2'5'ddU (100 μM) compared with that of Urd (100 μM) indicated that the 2'- and 5'-hydroxyl groups were not obligatory for transportability by hCNT1. Addition of an O-methyl group at the 2' position resulted in a substantial decrease of sodium current; with a concentration of 1 mM, only 41% of I_{Urd} induced by 100 μM Urd was observed with 2'OMeUrd. Although hCNT1 was able to transport Urd analogs with different modifications at C(2'), including substitution of the hydroxyl group with an azido group (2'AzdUrd), it barely transported AraU ($I_{\text{analog}}/I_{\text{Urd}} = 4.5\%$). hCNT1 exhibited high tolerance for substitution of the 5'-hydroxyl with chloro but lower tolerance for other substitutions (e.g., replacement with an azido or O-methyl group yielded poor permeants with $I_{\text{analog}}/I_{\text{Urd}}$ values of less than 10% of that observed with Urd). 3'dUrd initiated moderate to high inward currents at high concentrations ($I_{\text{analog}}/I_{\text{Urd}} = 91\%$, 3 mM of 3'dUrd, Fig. 3) and small but significant currents were induced by 3 mM of 2',3'ddUrd, 3',5'ddUrd, 3'AzdUrd, 3'MedUrdU and xyloU. No currents were observed in the presence of iPUrd.

hCNT2 transported Urd analogs with modifications at the C(2') position whereas those with modification at the C(5') and C(3') positions were poorly transported, if at all. Moderate currents were produced by 100 μM 2'dUrd while only small currents were induced by 3 mM 5'dUrd ($I_{\text{analog}}/I_{\text{Urd}} = 14.7\%$). Surprisingly, 2',5'ddU, a poor permeant for hCNT2 at 100 μM (3.1% of I_{Urd}), induced a higher current at a concentration of 3 mM than 5'dUrd. Similarly, although poor permeants at low concentrations, compounds with C(2') modifications initiated significant inward currents at higher concentration (3mM), with 2'AzdUrd > 2'OMeUrd > araU. C(5') modifications significantly reduced

transportability. hCNT2 transported 5'CldUrd and 5'AzdUrd poorly at high concentrations and was unable to transport 5'OMeUrd. Small and moderate currents were induced with 500 μ M and 3 mM 3'dUrd, respectively ($I_{\text{analog}}/I_{\text{Urd}} = 4.2\%$ at 500 μ M vs 30.4% at 3 mM). Although weak currents were detected with 3 mM 2'3'ddUrd, no currents were initiated by hCNT2 with xyloU, 3'5'ddU, 3'AzdUrd, 3'OMeUrd or iPUrd.

hCNT3 transported a board range of Urd analogs. The absence of the 2'- and/or 5'-hydroxyl groups had no effect on transportability by hCNT3 since the sodium currents produced by 100 μ M 2'Urd, 5'Urd and 2',5'ddUrd were similar to that of Urd (Fig. 3). At 50 μ M, the 2'AzdUrd-induced current was similar to that induced by 100 μ M Urd. However, hCNT3 showed reduced transportability of 2'OMeUrd ($I_{\text{analog}}/I_{\text{Urd}} = 33.6\%$ at 100 μ M and 64.5% at 1 mM). Moderate inward currents were induced by 3 mM araU, suggesting that the translocation pore of hCNT3 is more flexible than those of hCNT1 and hCNT2. Urd analogs containing 5' modifications, including 5'CldUrd, 5'AzdUrd and 5'OMeUrd, were good permeants with $I_{\text{analog}}/I_{\text{Urd}}$ of 29% for 10 μ M 5'CldUrd and about 70% for 5'AzdUrd and 5'OMeUrd. hCNT3 handled Urd analogs with 3' modifications much better than hCNT1 and hCNT2. Large currents were induced by 3'dUrd at 500 μ M ($I_{\text{analog}}/I_{\text{Urd}} = 77.5\%$). At high concentrations (3 mM), 3'dUrd (Fig. 3), 2',3'ddUrd and xyloU produced moderate to large inward currents whereas 3'AzdUrd, 3'OMeUrd and iPUrd induced low currents and thus were poor permeants of hCNT3.

Base and Sugar modifications. The hCNT1-mediated currents induced by FdUrd, BrdUrd, IdUrd and EtdUrd ($I_{\text{analog}}/I_{\text{Urd}} = 50\text{-}70\%$) were similar to those induced by FUrd, BrUrd and IUrd. The hCNT2-mediated current induced by FdUrd was reduced compared to that induced by 2'dUrd ($I_{\text{analog}}/I_{\text{Urd}} = 32.8\%$ for 100 μ M FdUrd vs 75.5% for 100 μ M 2'dUrd); current was also induced by BrdUrd whereas IdUrd and EtdUrd had almost no

MOL #12187

effect. FdUrd, BrdUrd and IdUrd all induced moderate currents in hCNT3-producing oocytes. Lack of the 5'-hydroxyl group in 5-fluoro-5'dUrd compared to 5FUrd had no effect on current induction in either hCNT1- or hCNT3-producing oocytes, but resulted in dramatically decreased currents in hCNT2-producing oocytes. Thd and AZT induced large and moderate currents, respectively, for hCNT1 and hCNT3 but very small or no currents for hCNT2.

Discussion

The present work used an improved yeast expressions system to characterize the Urd-binding motif of hCNT2. Among the three hCNT proteins, hCNT2 showed the lowest affinity for Urd and was most sensitive to modifications of its structure. The regions of the sugar moiety most critical for interaction with hCNT2 were the C(3')- and C(5')-OH groups. Retention of these two hydroxyl groups was required for high-affinity interactions with hCNT2 since all modifications at C(3') and C(5') reduced the capacity of hCNT2 to bind Urd analogs. The critical region of the base moiety of Urd for binding was identified as N(3)-H. The loss of more than 10.5 and 6.7 kJ/mol in Gibbs free energy, respectively, when the 3'- or 5'-hydroxyl groups and the N(3)-H were removed or modified suggested that these groups were involved in hydrogen bonding with hCNT2. These findings were consistent with the predictions of a recent computer-based pharmacophore model for nucleoside-hCNT2 binding, which suggested that hydrogen-bonding was a dominant determinate of interaction between hCNT2 and nucleosides (Chang et al., 2004).

The C(2') and C(5) positions were important regions for hCNT2 binding. hCNT2 tolerated the removal of the 2'-hydroxyl group but not its inversion of configuration or substitution with an azido or an O-methyl group. Considerable steric interference and physical separation introduced by modifications evidently weakened permeant-transporter interactions. Weak interactions, probably through Van der Waals forces, existed between hCNT2 and the C(5) position of the base moiety. Addition of halogen, methyl or ethyl groups to the C(5) regions of Urd and 2'dUrd resulted in similar affinity losses, roughly corresponding to the volume size of the modifications.

Although the structural regions of Urd that were involved in binding to hCNT2 shared similarities with those of hCNT1 and hCNT3, distinguishable features of hCNT2-Urd interactions were observed. We established previously that the 3'-hydroxyl is the single most critical functional group of Urd for high-affinity binding by hCNT1 and hCNT3 (Zhang et al., 2003); in this study we have found that both the 5'- and 3'-hydroxyl moieties were critical for hCNT2 binding. The C(2') and C(5) positions, which were relatively unimportant for hCNT1 or hCNT3 binding of Urd, were the second most important regions for hCNT2-Urd interactions. Multiple regions are required for direct or indirect hCNT2 interaction with Urd, suggesting that the amino acid residues composing the nucleoside-binding pocket of hCNT2 have limited selectivity for pyrimidine nucleosides.

Since the structural determinants of Urd that were identified by the inhibitor-sensitivity assay might not be equivalent to those required for physical translocation across the membrane by the hCNT proteins, the two-voltage clamp assay was used to determine the regions of Urd that were important for hCNT transportability in the *X. laevis* oocyte expression system. The regions of Urd required for hCNT1-mediated transport were identified as C(5), N(3) and C(3'). The transportability of Urd analogs depended on both the structural region(s) and the nature of the modifications. Urd analogs with C(5) modifications, which were high-affinity inhibitors of hCNT1 (Zhang et al., 2003), were also good permeants. Interestingly, a Urd analog with equal or even higher affinity than Urd did not necessarily produce higher currents than Urd. For example, hCNT1 exhibited significantly higher affinities for binding and transport of FUrd and FdUrd, since the apparent K_i and K_m values of FUrd and FdUrd were smaller than those of Urd (Smith et al., 2004; Zhang et al., 2003), however, the currents induced

by these two permeants were smaller than those induced by Urd. Methylation of N(3) reduced interactions with hCNT1 since the latter exhibited decreased affinity and greatly reduced transportability of 3MeUrd. C(2')-OH was not a determinant for hCNT1-uridine interactions since Urd analogs with modifications at this position were both good inhibitors (Zhang et al., 2003) and permeants of hCNT1. The 5'-hydroxyl group, which was previously identified as a potential H-bond donor for high affinity hCNT1-Urd interactions (Zhang et al., 2003), was not important for transport by hCNT1 because 5'dUrd and 5'ClUrd remained good permeants. However, 5'AzdUrd and 5'OMeUrd were not transported well by hCNT1, indicating that the 5' region of the sugar moiety contributes to permeant selectivity. Modifications at C(3') dramatically decreased the transportability of Urd analogs. hCNT1 was able to transport 3'dUrd and 2'3'ddUrd at very high concentrations but was unable to transport Urd analogs with bulkier C(3') substituents.

The transportability profile of hCNT2 corresponded well to its binding motif. Changes in almost all regions of Urd affected hCNT2 permeant selectivity. The most critical functional groups for binding to hCNT2 (i.e., the 3'- and 5'-hydroxyl groups) were also required for transportability. Almost any changes at the 3' or 5' positions, including removal of the hydroxyl group or inversion of configuration (at the 3' position), modification, or substitution, yielded Urd analogs that were poor permeants or not permeants at all. hCNT2 showed moderate affinity for 2'dUrd and also accepted 2'dUrd as a good permeant. Substitution of a variety of groups for the 2'-hydroxyl group yielded Urd analogs with poor binding in hCNT2-producing yeast and poor transport in hCNT2-producing oocytes. The N(3) region of Urd was also a determinant of transportability. The small volume of the C(5) region was evidently needed for tight binding and efficient

transport since substitution of H with bulkier groups resulted in a similarly large loss of both binding and transport.

The C(3'), C(5) and N(3) regions of Urd affected hCNT3 to different degrees. A potential hydrogen-bond interaction at C(3') of Urd was important for high-affinity binding and transport since removal or modification of the 3'-hydroxyl group significantly reduced analog binding and weakened transport. However, most poor inhibitors of hCNT3 protein appeared to be transported at high concentrations. The C(2') and C(5') regions of Urd, which were shown previously to be unimportant for Urd binding, were not important for transport since the C(2') and C(5') Urd analogs were also good permeants of hCNT3. Although modifications of C(5) and N(3) did not cause substantial changes in binding to hCNT3 (Zhang et al., 2003), the corresponding Urd analogs were transported less well than either Urd or 2'dUrd, suggesting that these two regions were minor determinants for hCNT3 transportability.

The transportability of Urd analogs by hCNT1, hCNT2 and hCNT3 reflected well the results obtained in the inhibitor-sensitivity assays. Most, if not all, of the Urd analogs that inhibited hCNT1, 2, or 3-mediated Urd transport were also permeants. hCNT2, which showed the least tolerance for modifications of Urd in the inhibitor-sensitivity assay, also exhibited limited transport of Urd analogs in the sodium flux assay. In contrast, hCNT3, with the 3'-hydroxyl group being the only important structural determinant for binding, showed good tolerance to various modifications of Urd with respect to transportability.

In summary, an improved yeast expression system was developed and used to determine the Urd binding motif of hCNT2, after which Urd analogs were applied to evaluate the transportability profiles of inhibitors of hCNT1, hCNT2 and hCNT3 with the

MOL #12187

two-electrode voltage clamp assay in oocytes of *X. laevis*. The transporters displayed key differences in their ligand recognition and permeant selectivities, indicating differences in permeant binding and translocation sites. Although poor inhibitors, 3'dUrd, 2',3'ddU, 3',5'ddU, araU, xyloU and AZT were permeants for hCNT1 and hCNT3 at high concentrations, indicating the important roles of these transporters for delivery and distribution of nucleoside analogs. The results of this work may guide the rational design of nucleoside drugs for use in the treatment of human diseases.

Acknowledgements

We thank Mrs. Pat Carpenter for her excellent technical assistance.

References

- Baldwin SA, Mackey JR, Cass CE and Young JD (1999) Nucleoside transporters: molecular biology and implications for therapeutic development. *Mol Med Today* **5**:216-24.
- Brunelli JP, Pall, M.L. (1993) A series of Yeast/*Escherichia coli* 1 expression vectors designed for directional cloning of cDNAs and *cre/lox*-Mediated Plasmid Excision. *Yeast* **9**:1309-18.
- Cass CE, Young JD, Baldwin SA, Cabrita MA, Graham KA, Griffiths M, Jennings LL, Mackey JR, Ng AML, Ritzel MWL, Vickers MF and Yao SYM (1999) Nucleoside Transporters of Mammalian Cells, in *Membrane Transporters as Drug Targets* (Amidon GL and Sadee W eds) pp 313-352, Kluwer Academic/Plenum Publishers.
- Chang C, Swaan PW, Ngo LY, Lum PY, Patil SD and Unadkat JD (2004) Molecular requirements of the human nucleoside transporters hCNT1, hCNT2, and hENT1. *Mol Pharmacol* **65**:558-70.
- Cheng Y and Prusoff WH (1973) Relationship between the inhibition constant (K_i) and the concentration of inhibitor which causes 50 per cent inhibition (I_{50}) of an enzymatic reaction. *Biochem Pharmacol* **22**:3099-108.
- de Koning HP and Jarvis SM (2001) Uptake of pentamidine in *Trypanosoma brucei* brucei is mediated by the P2 adenosine transporter and at least one novel, unrelated transporter. *Acta Trop* **80**:245-50.
- del Santo B, Tarafa G, Felipe A, Casado FJ and Pastor-Anglada M (2001) Developmental regulation of the concentrative nucleoside transporters CNT1 and CNT2 in rat liver. *J Hepatol* **34**:873-80.

- Garcia-Manteiga J, Molina-Arcas M, Casado FJ, Mazo A and Pastor-Anglada M (2003) Nucleoside transporter profiles in human pancreatic cancer cells: role of hCNT1 in 2',2'-difluorodeoxycytidine- induced cytotoxicity. *Clin Cancer Res* **9**:5000-8.
- Ito H, Fukuda Y, Murata K and Kimura A (1983) Transformation of intact yeast cells treated with alkali cations. *J Bacteriol* **153**:163-8.
- Jennings LL, Hao C, Cabrita MA, Vickers MF, Baldwin SA, Young JD and Cass CE (2001) Distinct regional distribution of human equilibrative nucleoside transporter proteins 1 and 2 (hENT1 and hENT2) in the central nervous system. *Neuropharmacology* **40**:722-31.
- Lang TT, Selner M, Young JD and Cass CE (2001) Acquisition of human concentrative nucleoside transporter 2 (hcnt2) activity by gene transfer confers sensitivity to fluoropyrimidine nucleosides in drug-resistant leukemia cells. *Mol Pharmacol* **60**:1143-52.
- Lang TT, Young JD and Cass CE (2004) Interactions of nucleoside analogs, caffeine, and nicotine with human concentrative nucleoside transporters 1 and 2 stably produced in a transport-defective human cell line. *Mol Pharmacol* **65**:925-33.
- Li JY, Boado RJ and Pardridge WM (2001) Differential kinetics of transport of 2',3'-dideoxyinosine and adenosine via concentrative Na⁺ nucleoside transporter CNT2 cloned from rat blood-brain barrier. *J Pharmacol Exp Ther* **299**:735-40.
- Mackey JR, Mani RS, Selner M, Mowles D, Young JD, Belt JA, Crawford CR and Cass CE (1998) Functional nucleoside transporters are required for gemcitabine influx and manifestation of toxicity in cancer cell lines. *Cancer Res* **58**:4349-57.

- Ngo LY, Patil SD and Unadkat JD (2001) Ontogenic and longitudinal activity of Na(+)-nucleoside transporters in the human intestine. *Am J Physiol Gastrointest Liver Physiol* **280**:G475-81.
- Patil SD, Ngo LY and Unadkat JD (2000) Structure-inhibitory profiles of nucleosides for the human intestinal N1 and N2 Na⁺-nucleoside transporters. *Cancer Chemother Pharmacol* **46**:394-402.
- Ritzel MW, Yao SY, Huang MY, Elliott JF, Cass CE and Young JD (1997) Molecular cloning and functional expression of cDNAs encoding a human Na⁺-nucleoside cotransporter (hCNT1). *Am J Physiol* **272**:C707-14.
- Ritzel MW, Yao SY, Ng AM, Mackey JR, Cass CE and Young JD (1998) Molecular cloning, functional expression and chromosomal localization of a cDNA encoding a human Na⁺/nucleoside cotransporter (hCNT2) selective for purine nucleosides and uridine. *Mol Membr Biol* **15**:203-11.
- Ritzel MWL, Ng AM, Yao SYM, Graham K, Loewen SK, Smith KM, Ritzel RG, Mowles DA, Carpenter P, Chen X, Karpinski E, Hyde RJ, Baldwin SA, Cass CE and Young JD (2001) Molecular identification and characterization of novel human and mouse concentrative Na⁺-Nucleoside cotransporter proteins (hCNT3 and mCNT3) broadly selective for purine and pyrimidine nucleosides (system *cib*). *J Biol Chem* **276**:2914-27.
- Smith KM, Ng AM, Yao SY, Labeledz KA, Knaus EE, Wiebe LI, Cass CE, Baldwin SA, Chen XZ, Karpinski E and Young JD (2004) Electrophysiological characterization of a recombinant human Na⁺-coupled nucleoside transporter (hCNT1) produced in *Xenopus* oocytes. *J Physiol* **558**:807-23.

- Vickers MF, Kumar R, Visser F, Zhang J, Charania J, Raborn RT, Baldwin SA, Young JD and Cass CE (2002) Comparison of the interaction of uridine, cytidine, and other pyrimidine nucleoside analogues with recombinant human equilibrative nucleoside transporter 2 (hENT2) produced in *Saccharomyces cerevisiae*. *Biochem Cell Biol* **80**:639-44.
- Vickers MF, Mani RS, Sundaram M, Hogue DL, Young JD, Baldwin SA and Cass CE (1999) Functional production and reconstitution of the human equilibrative nucleoside transporter (hENT1) in *Saccharomyces cerevisiae*. Interaction of inhibitors of nucleoside transport with recombinant hENT1 and a glycosylation-defective derivative (hENT1/N48Q). *Biochem J* **339**:21-32.
- Vickers MF, Yao SY, Baldwin SA, Young JD and Cass CE (2000) Nucleoside transporter proteins of *Saccharomyces cerevisiae*. Demonstration of a transporter (FUI1) with high uridine selectivity in plasma membranes and a transporter (FUN26) with broad nucleoside selectivity in intracellular membranes. *J Biol Chem* **275**:25931-8.
- Vickers MF, Zhang J, Visser F, Tackaberry T, Robins MJ, Nielsen LP, Nowak I, Baldwin SA, Young JD and Cass CE (2004) Uridine recognition motifs of human equilibrative nucleoside transporters 1 and 2 produced in *Saccharomyces cerevisiae*. *Nucleosides Nucleotides Nucleic Acids* **23**:361-73.
- Visser F, Zhang J, Raborn RT, Baldwin SA, Young JD and Cass CE (2005) Residue 33 of human equilibrative nucleoside transporter 2 is a functionally important component of both the dipyridamole and nucleoside binding sites. *Mol Pharmacol* **67**:1291-8.
- Winzler EA, Shoemaker DD, Astromoff A, Liang H, Anderson K, Andre B, Bangham R, Benito R, Boeke JD, Bussey H, Chu AM, Connelly C, Davis K, Dietrich F, Dow SW, El Bakkoury M, Foury F, Friend SH, Gentalen E, Giaever G, Hegemann JH, Jones

MOL #12187

T, Laub M, Liao H, Davis RW and et al. (1999) Functional characterization of the *S. cerevisiae* genome by gene deletion and parallel analysis. *Science* **285**:901-6.

Zhang J, Visser F, Vickers MF, Lang T, Robins MJ, Nielsen LP, Nowak I, Baldwin SA, Young JD and Cass CE (2003) Uridine binding motifs of human concentrative nucleoside transporters 1 and 3 produced in *Saccharomyces cerevisiae*. *Mol Pharmacol* **64**:1512-20.

Footnotes

This research was funded by the National Cancer Institute of Canada (C.E.C and J.D.Y.), Alberta Cancer Board (C.E.C. and J.D.Y.), and pharmaceutical company gift funds to Brigham Young University (M.J.R.). C.E.C. is Canada Research Chair in Oncology and J.D.Y. is Heritage Scientist of the Alberta Heritage Foundation for Medical Research. Studentship support was from the Canadian Institute of Health Research (J.Z.), the Alberta Heritage Foundation for Medical Research (J.Z. and F.V.), the Department of Oncology Endowed Studentship (J.Z. and F.V.), and the Brigham Young University Undergraduate Research Fellowship (L.P.C.N.).

Reprint requests to: Dr. Carol E. Cass, Department of Oncology, University of Alberta, Cross Cancer Institute, 11540 University Ave., Edmonton, Alberta, Canada T6H 1Z2 (Tel: 780-432-8320; Fax: 780-432-8425; email: carol.cass@cancerboard.ab.ca)

From the Membrane Protein Research Group (J.Z., K.M.S., T.T., F.V., J.D.Y. and C.E.C.), Departments of Oncology (J.Z., T.T., F.V. and C.E.C.) and Physiology (K.M.S., E.K. and J.D.Y.), University of Alberta, and the Cross Cancer Institute (J.Z., T.T., F.V. and C.E.C.), Edmonton, Alberta T6H 1Z2, Canada, the Department of Chemistry and Biochemistry (M.J.R., L.P.C.N. and I.N.), Brigham Young University, Provo UT 84602-5700, USA, and the ⁴School of Biochemistry and Molecular Biology (S.A.B.), University of Leeds, Leeds LS2 9JT, United Kingdom

Figure legends

Fig. 1. Immunoblotting detection and functional characterization of recombinant hCNT2 in yeast. **A. Immunoblotting.** Yeast (*fui1::HIS3*) were transformed with either pYPGE15 or pYPhCNT2 to form new yeast strains named *fui1::HIS3* + pYPGE15 and *fui1::HIS3* + pYphCNT2. Yeast membranes (20 μ g protein) were subjected to SDS-polyacrylamide gel electrophoresis, after which proteins were transferred to polyvinylidene fluoride membranes that were subjected to immunoblotting with anti-hCNT2 monoclonal antibodies. The positions of the molecular mass markers are indicated in kDa at the right. **B. Time courses of [³H]Urd uptake.** The uptake of 1 μ M [³H]Urd by yeast that were transformed with pYphCNT2 was measured in CMM/GLU (pH 7.4) in the presence of 100 mM NaCl, either alone (close symbols) or with 10 mM non-radioactive Urd (open symbols). **C. Kinetic properties.** The mediated component of Urd transport (uptake rates of [³H]Urd at a particular Urd concentration minus uptake rates at that concentration in the presence of 10 mM non-radioactive permeants) was plotted as a function of concentration and subsequently converted to *V versus V/S* plots (insets) to determine the kinetic constants for the hCNT2 (PRISM, GraphPad Software). Each value is the mean \pm S.E. of 9 determinations and S.E. values are not shown where they were smaller than the data points. Each graph represents one of three identical experiments that gave qualitatively similar results.

Fig. 2. Inhibition of recombinant hCNT2-mediated Urd uptake by some Urd analogs. The uptake of 1 μ M [³H]Urd into *fui1::HIS3* yeast producing hCNT2 was measured over 20 min in the presence of graded concentrations of test compounds. The

test compounds were: Urd (■), 2'dUrd (▽), 3'dUrd (△), 5FUrd (◆), 3'AzdUrd (*), FdUrd (●), EtdUrd (○), MeUrd (▲), IUrd (◇), 2'AzdUrd (□), 2'OMeUrd (+), and 5'CldUrd (▼). Uptake values in the presence of Urd compounds are given as the percentage of uptake values in their absence. Each data point represents the means \pm S.E. of quadruplicate determinations; error bars are not shown where they are smaller than the symbol. Three or four independent experiments gave similar results and results from representative experiments are shown.

Fig. 3. Representative sodium currents in the presence of Urd, 2'dUrd, 3'dUrd or 5'dUrd. Oocytes were injected with 10 nl of water without (control) or with 10 ng of hCNT1, hCNT2 or hCNT3 transcripts. The expression vector was pGEM-HE. Current responses were generated by perfusing individual hCNT1, 2 or 3-producing oocytes with either 2'dUrd, 3'dUrd or 5'dUrd with the concentrations as indicated in a sodium-containing transport medium (top three panels). The current produced by 100 μ M Urd in a sodium-containing medium is shown for comparison. The same experiment was performed in a control water-injected oocyte (bottom panel). Structures were drawn using ChemDraw Ultra version 6.0 software and numbering for Urd is indicated .

Fig. 4. Transport of Urd and Urd analogs by hCNT1, hCNT2 and hCNT3. Currents were generated by perfusing hCNT1, 2 or 3-producing oocytes with Urd or various Urd analogs with base modifications (concentrations as indicated) in a sodium-containing medium. Values are means \pm S.E. for 3 different oocytes. The same experiment was also performed in control water-injected oocytes (data not shown); no inward currents were generated. The expression vector was pGEM-HE.

Table 1 K_i and Gibbs free energy values for inhibition of hCNT2-mediated Urd uptake in *Saccharomyces cerevisiae* by Urd analogs

Urd compounds	IC ₅₀ (μM)	K _i (μM)	ΔG ⁰	(δ(ΔG ⁰))
Urd	29 ± 3	28 ± 3	23.8	0
Base modification				
5-fluorouridine (FUrd)	63 ± 13	61 ± 13	22.1	1.7
5-iodouridine (IUrd)	371 ± 51	358 ± 50	18.1	5.7
5-bromouridine (BrUrd)	238 ± 4	230 ± 4	19.1	4.7
5-methyluridine (MeUrd)	165 ± 0.3	160 ± 1	19.9	3.9
3-methyluridine (3MeUrd)	581 ± 151	562 ± 146	17.1	6.7
Sugar modification				
2'-deoxyuridine (2'dUrd)	76 ± 8	73 ± 8	21.7	2.1
5'-deoxyuridine (5'dUrd)	> 3000*	> 3000*	< 13.3	> 10.5
3'-deoxyuridine (3'dUrd)	> 3000 ⁺	> 3000 ⁺		
1-(β-D-arabinofuranosyl)uracil (araU)	> 3000*	> 3000*		
1-(β-D-xylofuranosyl)uracil (xyloU)	> 3000*	> 3000*		
2',5'-dideoxyuridine (2',5'ddUrd)	> 3000*	> 3000*		
3',5'-dideoxyuridine (3',5'ddUrd)	> 3000*	> 3000*		
2',3'-dideoxyuridine (2',3'ddUrd)	> 3000 ⁺	> 3000 ⁺		
2'-O-methyluridine (2'OMeUrd)	> 1000*	> 1000*	< 15.8	> 8.0
5'-O-methyluridine (5'OMeUrd)	> 3000*	> 3000*		
3'-O-methyluridine (3'OMeUrd)	> 3000*	> 3000*		
2'-azido-2'-deoxyuridine (2'AzdUrd)	> 3000 ⁺	> 3000 ⁺		
3'-azido-3'-deoxyuridine (3'AzdUrd)	> 3000*	> 3000*		
5'-azido-5'-deoxyuridine (5'AzdUrd)	> 3000*	> 3000*		
5'-chloro-5'-deoxyuridine (5'ClUrd)	> 1000*	> 1000*		
2',3'-O-isopropylideneuridine (iPUrd)	> 3000*	> 3000*		
Base & sugar modifications				
5-fluoro-2'-deoxyuridine (FdUrd)	156 ± 7	151 ± 7	20.0	3.8
5-bromo-2'-deoxyuridine (BrdUrd)	272 ± 75	263 ± 72	18.8	5.0
5-iodo-2'-deoxyuridine (IdUrd)	303 ± 20	293 ± 11	18.5	5.3
5-ethyl-2'-deoxyuridine (EtdUrd)	353 ± 40	341 ± 39	18.2	5.6
5-fluoro-5'-deoxyuridine	> 3000 ⁺	> 3000 ⁺		
Thymidine (Thd)	586 ± 20	566 ± 20	17.0	6.8
3'-azido-3'-deoxythymidine (AZT)	> 3000 ⁺	> 3000 ⁺		

* No obvious inhibition was observed.

+ Inhibition of less than 50% was observed.

The uptake of 1 μM [^3H]Urd into yeast (*fui1::HIS3*) expressing pYPhCNT2 was measured over 20 min in the presence of graded concentrations of non-radioactive Urd or Urd analogs. IC_{50} values (mean \pm S.E., $n = 3-4$) were determined using Graphpad Prism Version 3.0 Software and were converted to K_i values (Cheng and Prusoff, 1973) using K_m values (mean \pm S.E., $n = 3$) of $29 \pm 7 \mu\text{M}$ for recombinant hCNT2. Gibbs free energy (ΔG^0) was calculated from $\Delta G^0 = -RT\ln(K_i)$.

Table 2 The transportability of uridine analogs by hCNT1, hCNT2 and hCNT3 as measured by induction of sodium currents.

Uridine analogs	Concentration (μM)	$I_{\text{Analog}}/I_{\text{Urd}}$ (% of value observed with 100 μM Urd)		
		hCNT1	hCNT2	hCNT3
Urd	100	100 \pm 8.0	100 \pm 9.2	100 \pm 14.4
Base modifications				
IUrd	10	21.5 \pm 2.6	1.2 \pm 0.6	25.6 \pm 1.2
IUrd	500	60.6 \pm 3.1	12.4 \pm 2.1	54.9 \pm 3.4
MeUrd	100	66.6 \pm 11.5	8.5 \pm 0.7	55.5 \pm 4.8
MeUrd	500	72.5 \pm 5.7	24.9 \pm 3.2	59.3 \pm 8.8
FUrd	50	50.2 \pm 4.7	30.0 \pm 4.0	45.6 \pm 4.7
FUrd	100	66.3 \pm 4.6	43.9 \pm 3.0	44.2 \pm 4.6
BrUrd	100	59.9 \pm 5.6	4.3 \pm 0.7	60.3 \pm 6.9
BrUrd	500	61.6 \pm 4.7	11.4 \pm 1.6	71.8 \pm 9.9
3MeUrd	100	0.5 \pm 0.3	2.4 \pm 0.6	4.6 \pm 0.9
3MeUrd	500	3.8 \pm 1.2	10.2 \pm 0.2	48.4 \pm 4.4
Sugar modifications				
2'dUrd	10	18 \pm 3.6	16.8 \pm 2.1	30.5 \pm 2.5
2'dUrd	100	62.1 \pm 9.0	75.5 \pm 10.4	99.9 \pm 7.8
5'dUrd	50	39.6 \pm 6.3	1.0 \pm 0.7	85.4 \pm 3.5
5'dUrd	3000	218.9 \pm 18.9	14.7 \pm 2.1	150.9 \pm 6.0
3'dUrd	500	39.6 \pm 4.5	4.2 \pm 2.0	75.4 \pm 4.6
3'dUrd	3000	91 \pm 9.9	30.4 \pm 6.3	107.3 \pm 6.4
araU	3000	4.5 \pm 1.8	13.6 \pm 1.5	52.1 \pm 2.5
xyloU	3000	9.9 \pm 1.8	0	62.3 \pm 3.9
2',5'ddU	100	111.7 \pm 7.2	3.1 \pm 1.2	100.9 \pm 4.6
2',5'ddU	3000	166.6 \pm 12.6	46.2 \pm 7.3	117.6 \pm 14.6
3',5'ddU	3000	11.7 \pm 2.7	0	29.8 \pm 3.2
2',3'ddU	3000	54.9 \pm 12.6	2.1 \pm 1.0	87.8 \pm 6.0
2'OMeUrd	100	23.4 \pm 3.6	5.2 \pm 1.2	33.6 \pm 3.9
2'OMeUrd	1000	41.4 \pm 5.4	29.4 \pm 5.3	64.5 \pm 5.7
5'OMeUrd	100	8.1 \pm 2.7	0	63 \pm 8.1
5'OMeUrd	3000	46.8 \pm 5.4	0	79 \pm 10.2
3'OMeUrd	3000	4.5 \pm 1.8	0	12 \pm 1.1
2'AzdUrd	50	28.8 \pm 7.2	8.4 \pm 2.0	75.8 \pm 3.9
2'AzdUrd	3000	N.D.	39.9 \pm 4.2	N.D.
3'AzdUrd	1000	0	N.D.	6.4 \pm 1.4
3'AzdUrd	3000	3.6 \pm 1.8	0	16.3 \pm 2.5
5'AzdUrd	100	9.0 \pm 2.7	N.D.	78.6 \pm 4.3
5'AzdUrd	3000	N.D.	25.2 \pm 3.1	N.D.
5'ClUrd	10	18.9 \pm 1.8	0	29 \pm 1.8
5'ClUrd	1000	149.5 \pm 11.7	31.5 \pm 8.4	147.7 \pm 10.6
iPUrd	3000	0	0	2.5 \pm 0.7
Base and sugar modifications				
FdUrd	10	22.2 \pm 1.4	4.4 \pm 0.5	31.8 \pm 5.5
FdUrd	100	72.3 \pm 5.0	32.8 \pm 4.7	81.3 \pm 18.8
BrdUrd	10	20.3 \pm 2.4	2.1 \pm 0.6	23.4 \pm 3.2
BrdUrd	500	56.3 \pm 9.0	32.6 \pm 7.0	N.D.
IdUrd	100	72.1 \pm 3.8	1.0 \pm 0.3	54.9 \pm 6.2
EtdUrd	50	51.4 \pm 4.1	0.3 \pm 0.3	51.5 \pm 3.1
EtdUrd	500	113.5 \pm 11.8	2.3 \pm 0.1	70.6 \pm 2.5
5-fluoro-5'dUrd	50	33.4 \pm 0.8	0.0	37.7 \pm 2.0
5-fluoro-5'dUrd	3000	N.D.	12.4 \pm 2.1	N.D.
Thd	100	83.2 \pm 2.8	4.1 \pm 1.4	63.1 \pm 10.6
AZT	100	19.2 \pm 1.7	0.0	8.5 \pm 1.3
AZT	1000	59.9 \pm 6.5	0.0	28.1 \pm 3.2

Oocytes producing hCNT1, 2 or 3 were voltage-clamped at -50 mV in a sodium-containing medium and currents were measured in the presence of Urd analogs at different concentrations (3-4 different oocytes per assay). The mean values of Urd analog-induced currents were normalized to the mean value of Urd-produced currents (100 μ M of Urd) and summarized as $I_{\text{Analog}}/I_{\text{Urd}}$. None of the Urd analogs induced currents in water-injected control oocytes (data not shown). The expression vector was pGEM-T. N.D., not determined.

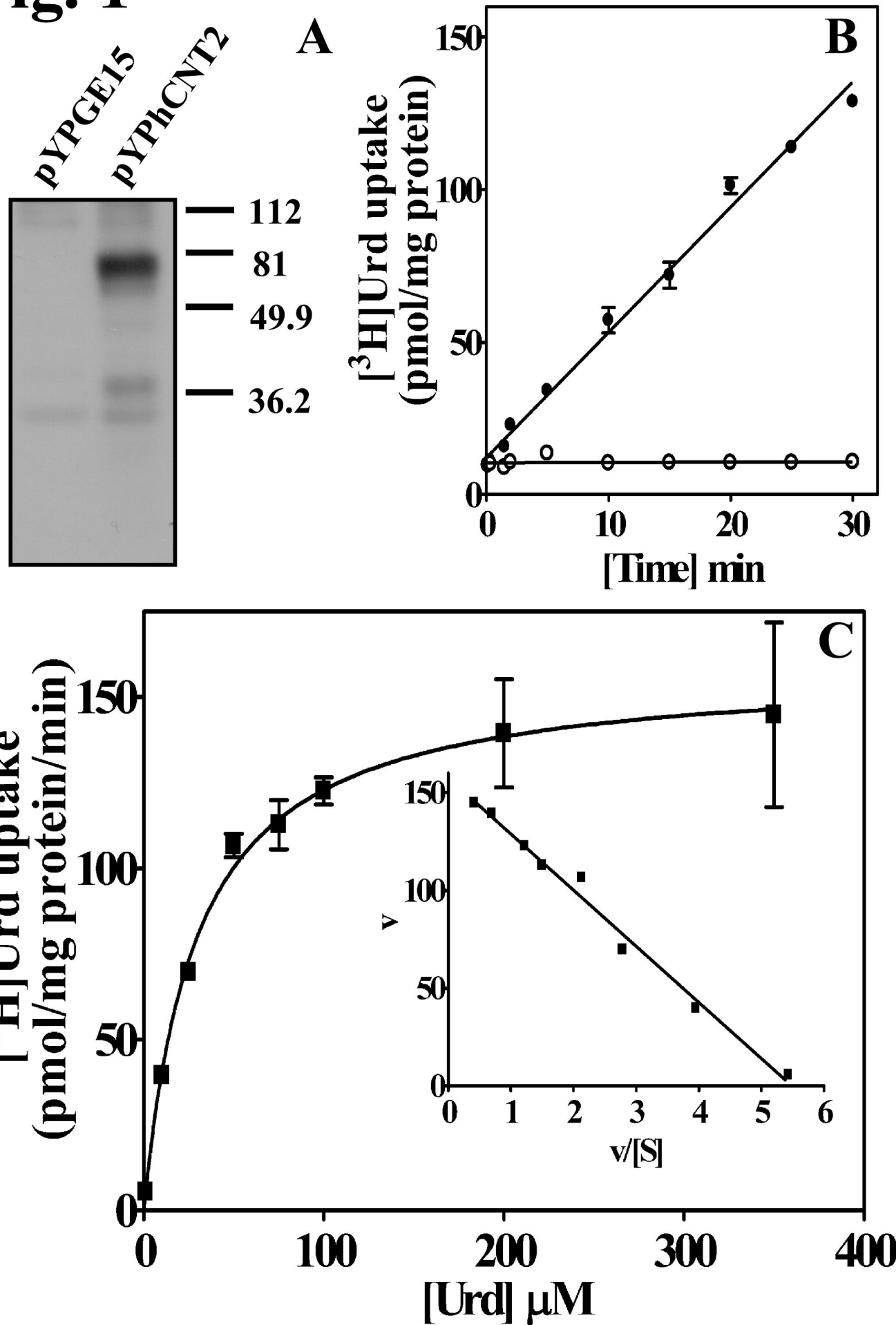
Fig. 1

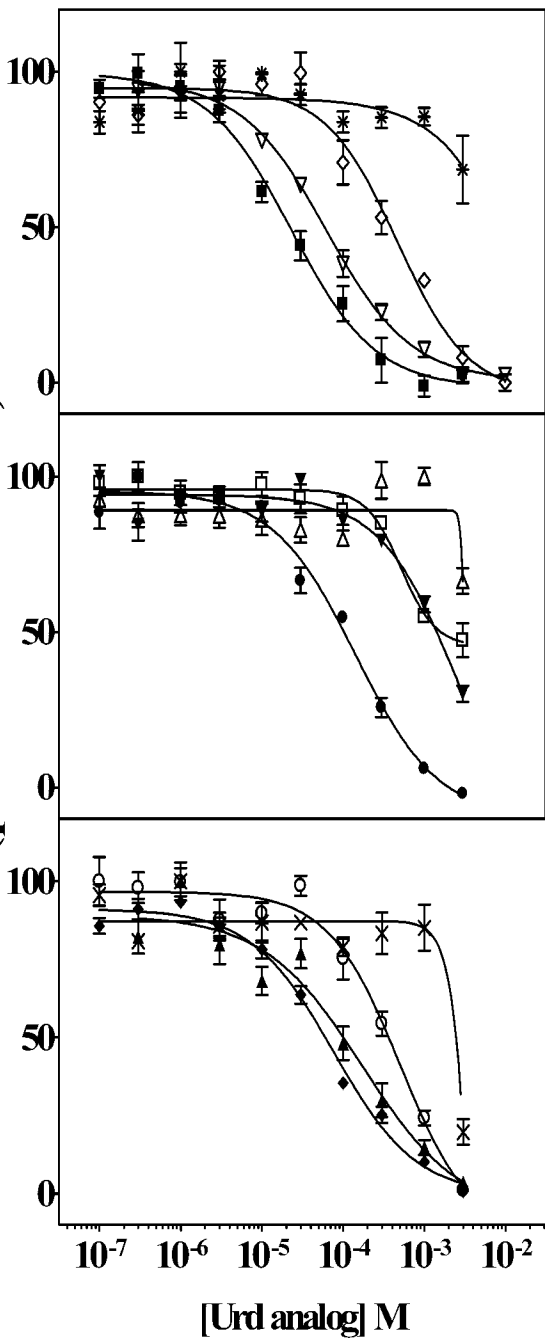
Fig. 2**1 μ M [3 H]Urd uptake
(percent of control)**

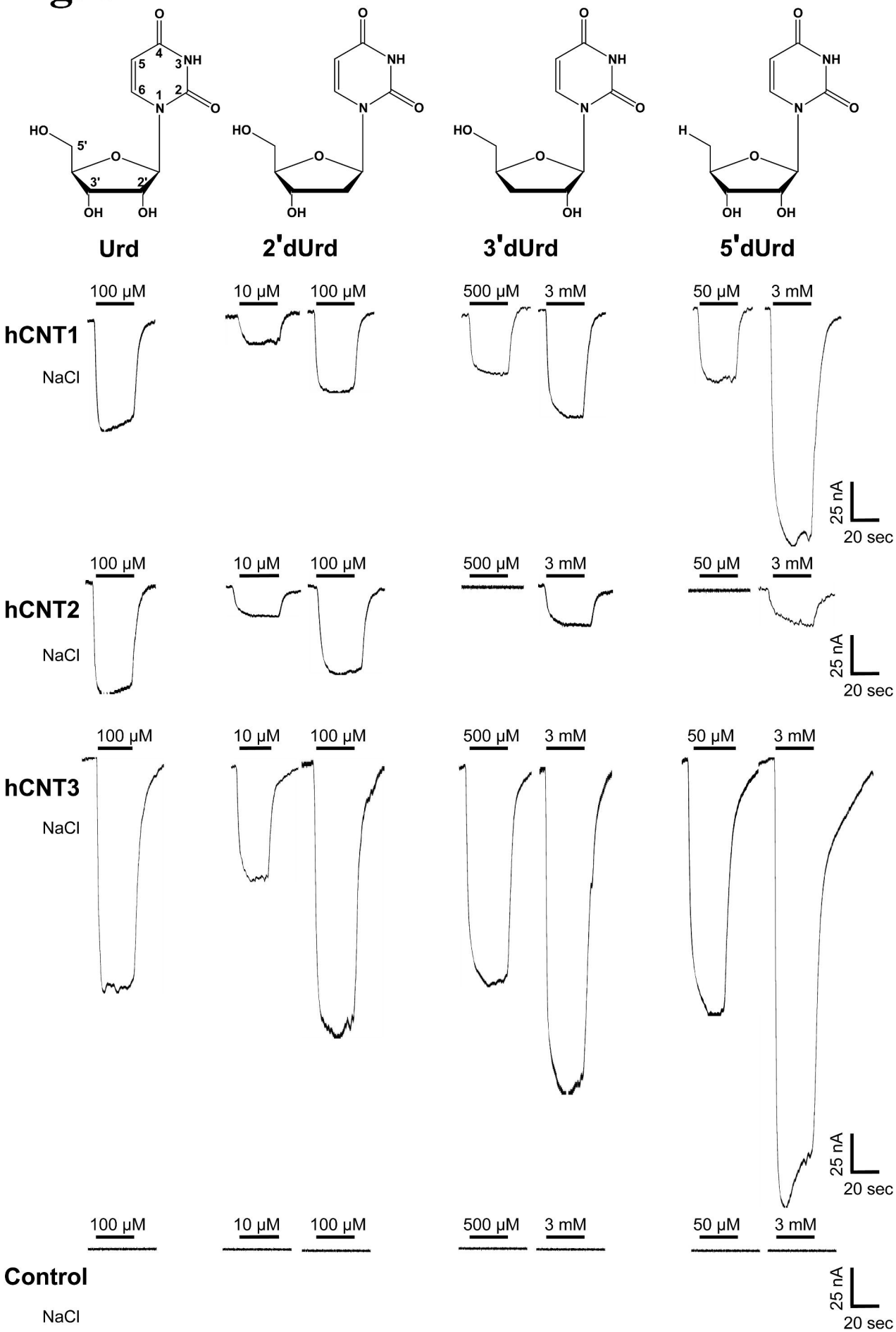
Fig. 3

Fig. 4

